Probing the Folding Mechanism of a Leucine Zipper Peptide by Stopped-Flow Circular Dichroism Spectroscopy†

Jill A. Zitzewitz, Osman Bilsel, Jiabin Luo, Bryan E. Jones,‡ and C. Robert Matthews*

Department of Chemistry and Center for Biomolecular Structure and Function, The Pennsylvania State University, University Park, Pennsylvania 16802

Received June 29, 1995; Revised Manuscript Received August 17, 1995®

ABSTRACT: Leucine zipper peptides provide simple model systems for studying both the intramolecular and intermolecular interactions that govern protein folding. The synthetic 33-residue peptide GCN4-p1, derived from the yeast transcriptional activator GCN4, forms a stable bimolecular coiled-coil structure [O'Shea, E. K., Klemm, J. D., Kim, P. S., & Alber, T. (1991) *Science 254*, 539−544]. The guanidine-HCl induced equilibrium unfolding of this peptide at 5 °C and pH 7.0 yields a standard state free energy of 10.49 ± 0.23 kcal (mol dimer)$^{-1}$ when fit to a two-state model involving the native dimer and the unfolded monomer. The unfolding and refolding kinetics of GCN4-p1 were monitored by stopped-flow circular dichroism spectroscopy as a function of both peptide concentration and final denaturant concentration. The unfolding kinetics displayed single-exponential behavior, consistent with a unimolecular reaction. The refolding kinetics, which are dependent on both peptide and guanidine concentration, are well described by a simple bimolecular association reaction. A simultaneous fit of all of the unfolding and refolding kinetic data to the model, $N_2 \underset{k_f}{\overset{k_u}{\rightleftharpoons}} 2U$, yields refolding and unfolding rate constants in the absence of denaturant of 4.2×10^5 M^{-1} s^{-1} and 3.3×10^{-3} s^{-1}, respectively. The equilibrium unfolding curve is accurately predicted from these rate constants, providing further support for the validity of the two-state kinetic model.

Protein folding is a remarkably complex process in which an ensemble of random, interconverting structures are guided to a unique, native structure by a multitude of noncovalent interactions between backbone and side-chain atoms. Much of the progress toward understanding how the amino acid sequence of a protein directs this rapid and efficient conformational transition has been achieved by analysis of the folding of monomeric proteins (Kim & Baldwin, 1990; Matthews, 1993). These studies, however, do not address the question of how monomers self-assemble into higher order structures, i.e., how quaternary structure develops in multisubunit proteins. Although the folding of oligomeric proteins has been the subject of numerous thermodynamic and kinetic studies [for reviews, see Jaenicke (1987, 1991) and Garel (1992) and, for selected examples, see Zetina and Goldberg (1982), Blond and Goldberg (1985), and Ziegler et al. (1993)], the structural complexity of many of these systems has made it difficult to elucidate the mechanistic features of the association reaction. A few small dimeric proteins have been studied in an effort to simplify this problem, including the *trp* aporepressor (Gittelman & Matthews, 1990; Mann & Matthews, 1993) and the P22 *arc* repressor (Milla & Sauer, 1994; Schildbach et al., 1995). Even these small proteins, however, contain multiple elements of secondary structure whose formation and intramolecular associations complicate the study of quaternary structure formation.

The parallel two-stranded coiled-coil domain appears to offer the simplest system for studying both the intra- and intermolecular interactions which govern the folding and stability of multisubunit proteins. Coiled-coil proteins are the basic structural element of many fibrous proteins (Cohen & Parry, 1986) and also occur in membrane-spanning proteins (Cohen & Parry, 1990) and transcription factors (Ellenberger, 1994). The coiled-coil structure, which was first postulated by Crick (1953), is formed by two right-handed α-helices that wrap around each other at a 20° angle to form a left-handed superhelix with a superhelical pitch of ~140 Å. The structural repeat unit in each helix is a heptapeptide, $(abcdefg)_n$. Hydrophobic residues in the *a* and *d* positions and oppositely charged residues in the *e* and *g* positions together form the contact surface between the individual amphipathic helices. The interactions which stabilize coiled coils are now well-understood as a consequence of (1) thermodynamic studies of naturally occurring proteins (Lehrer, 1978; Holtzer et al., 1983; O'Shea et al., 1989), (2) the design and characterization of many simple peptide models of diverse length and sequence (DeGrado, 1988; Regan & DeGrado, 1988; Monera et al., 1993; Zhou et al., 1994; Rozzelle et al., 1994; Myszka & Chaiken, 1994; Munson et al., 1994), and (3) the determination of the crystal structures of several leucine zipper peptides (O'Shea et al., 1991; Harbury et al., 1993; Harbury et al., 1994). Information on the mechanistic details of the kinetics of coiled-coil formation, however, is still limited.

The first mechanistic analysis of coiled-coil formation involved stopped-flow circular dichroism refolding studies

† This work was supported by NIH Grant GM 23303 and NSF Grant MCB 9317273 to C.R.M. and NIH Grant GM 14954 to J.A.Z.

* Author to whom correspondence should be addressed.

‡ Present address: Department of Biochemistry, University of Washington, Seattle, WA 98195.

® Abstract published in *Advance ACS Abstracts,* October 1, 1995.

0006-2960/95/0434-12812$09.00/0

on the fibrous protein tropomyosin (Mo et al., 1991a,b). The association of the 284 residue monomer chains was shown to occur during the dead-time of mixing (<40 ms) over a 100-fold protein concentration range (0.05−5.0 mg mL^{-1}). The observed dimeric intermediate displays approximately 70% of the native CD[1] signal and folds to the native structure by a first order reaction. More recently, Bosshard and coworkers have studied the formation of coiled-coil structure in small leucine zipper peptides by attaching a fluorescent probe to the amino termini of the peptides through a triglycine spacer (Wendt et al., 1994, 1995). In one set of experiments, the folding reaction of GCN4-p1, which represents the coiled-coil domain of GCN4, was probed by monitoring the self-quenching of the fluorescence signal observed after small perturbations in a pre-existing equilibrium (Wendt et al., 1994). At least one, and possibly two, first-order conformational rearrangements were proposed to occur after association of the monomer chains. As was the case in the refolding of tropomyosin, a concentration-dependent association step was not directly observed. In a subsequent similar experiment involving the folding of a series of engineered leucine zipper peptides, a bimolecular association step on the order of 10^6 M^{-1} s^{-1} was observed and, in some cases, was coupled to a unimolecular conformational reorganization (Wendt et al., 1995). Not addressed in these fluorescence studies was the issue of secondary structure formation and its relationship to the association reaction.

A useful approach to the mechanistic characterization of the kinetics of coiled-coil formation involves the application of stopped-flow circular dichroism to monitor the folding of leucine zipper peptides. Because far-UV CD provides a global probe of secondary structure, this technique has the potential to monitor the formation of structure in the individual monomers as well as in the folded, dimeric form. Mechanistic details of the folding reaction can be obtained by studying the unfolding and refolding kinetics at various final concentrations of peptide and/or chemical denaturant. The leucine zipper peptide, GCN4-p1, from the yeast transcriptional activator GCN4, was selected as a model system because the native structure of this 33-residue peptide has been well characterized by both NMR (Oas et al., 1990; Goodman & Kim, 1991) and X-ray crystallography (O'Shea et al., 1991) and has been shown to form a well-defined, two-stranded, parallel coiled-coil structure.

Thermodynamic and kinetic analyses of the Gdn-HCl-induced unfolding and refolding of the GCN4-p1 dimer, as probed by CD, show that this simple system is well-described by a two-state model. Only the native dimer and unfolded monomer are required to explain the equilibrium and kinetic behavior of this peptide. The simplicity of this system lends itself to quantitative assessments of the factors which direct the formation of quaternary structure.

MATERIALS AND METHODS

Peptide Purification. The synthetic GCN4-p1 peptide Ac-RMKQLEDKVEELLSKNYHLENEVARLKKLVGER-$CONH_2$ (a gift from S. Marqusee) was purified by reverse-phase HPLC at room temperature on a Vydac (Hesperia, CA) semipreparative C18 column. A 12 min isocratic elution in 10% acetonitrile and 0.1% TFA was followed by a gradient from 10% to 70% acetonitrile in 0.1% TFA over 45 min at a flow rate of 2 mL min^{-1}. The purified peptide (retention time = 44 min) was concentrated at 4 °C in a Savant Speed Vac Concentrator to remove the acetonitrile and then lyophilized twice from water to remove residual TFA. The purity of the peptide was confirmed by the presence of a single peak on an analytical reverse-phase HPLC chromatogram. The integrity of the peptide was further confirmed by electrospray mass spectrometry, which yielded a molecular weight of 4038.9 (MW_{calc} = 4038.7).

Reagents and Experimental Conditions. Ultrapure guanidine HCl was purchased from ICN Biomedicals, Inc. (Costa Mesa, CA) and used without further purification. All other chemicals were reagent grade. Folding experiments were carried out at a temperature of 5 °C in buffer solutions containing 50 mM sodium phosphate, 150 mM NaCl, and 1 mM β-mercaptoethanol at pH 7.0. Peptide concentrations were measured in 6 M Gdn-HCl from the tyrosine absorbance at 276 nm, using an extinction coefficient of 1500 M^{-1} cm^{-1} (Edelhoch, 1967).

Circular Dichroism Spectroscopy. Equilibrium CD experiments were performed on an Aviv 62DS spectrometer equipped with a Hewlett Packard 89100A temperature controller. Samples were prepared by diluting 100 μL of a stock peptide solution into 600 μL of buffer containing various concentrations of Gdn-HCl (0−7 M). The samples were equilibrated at 5 °C for 1 h prior to collecting data. The samples were shown to be fully equilibrated by the absence of further changes in the CD signal at longer equilibration times. All CD spectra were taken from 300 to 200 nm using a 2.0 s averaging time, a 1.0 nm step size, and a 2.0 mm path length cell.

Stopped-flow kinetic data were obtained using a Biologic SFM-3 stopped-flow attachment mounted on the Aviv CD spectrometer. A circulating water bath was used to maintain the temperature in the cell holder and syringe reservoirs at 5 °C. Refolding was initiated by a rapid 10-fold dilution of peptide in 5 M Gdn-HCl with buffer or Gdn-HCl solutions at a flow rate of 5 mL s^{-1}. The dead-time of mixing for the refolding experiments was 5 ms (Mann & Matthews, 1993). Only two syringes were utilized for unfolding jumps: peptide in buffer was rapidly diluted 5-fold into various concentrations of Gdn-HCl. The dead-time for the unfolding experiments was determined to be 14 ms by measuring the reduction of 2,6-dichlorophenolindophenol by L-ascorbic acid (Tonomura et al., 1978). For all kinetic experiments, the detection wavelength was 222 nm, and the cell path length was 2.0 mm. Data collections were made over two separate time domains: (1) 2 or 5 s using an instrumental time constant of 1 ms and (2) 20 or 50 s using a time constant of 10 ms. Typically, the results of 20−40 syringe firings were averaged for each kinetic trace.

Data Analysis. Equilibrium curves were fit to the two-state model

$$N_2 \overset{K}{\rightleftharpoons} 2U \qquad (1)$$

where N_2 is the native peptide dimer, U is the unfolded monomer, and $K = [U]^2/[N_2]$. Assuming this model, the apparent fraction of the unfolded form, $F_{app} = (\theta_O - \theta_N)/$

[1] Abbreviations: CD, circular dichroism; GCN4-p1, synthetic peptide corresponding to residues 249−281 of the transcriptional activator GCN4; Gdn-HCl, guanidine hydrochloride; HPLC, high-performance liquid chromatography; TFA, trifluoroacetic acid; UV, ultraviolet.

($\theta_U - \theta_N$), is (Gittelman & Matthews, 1990; Mann & Matthews, 1993):

$$F_{app} = \frac{(K^2 + 8K[P_{tot}])^{1/2} - K}{4[P_{tot}]} \quad (2)$$

where $[P_{tot}] = 2[N_2] + [U]$ is the total peptide concentration expressed in terms of monomer. The free energy of unfolding in the absence of denaturant was obtained by assuming a linear dependence of the apparent free energy diffference on denaturant concentration (Schellman, 1978; Pace, 1986). The ellipticity at 222 nm as a function of Gdn-HCl concentration was fit using a nonlinear least-squares analysis program, NLIN (SAS Institute, Inc., Cary, NC), assuming that the ellipticities of the unfolded and native forms also depend linearly on denaturant concentration. A global analysis of all of the peptide concentration-dependent equilibrium data was obtained using in-house software, where the free energy of unfolding and the slopes of the unfolded and native baseline regions were linked parameters.

The kinetic data were fit locally or globally (Knutson et al., 1983) with in-house software using either the Marquardt (Marquardt, 1963) or simplex (Press et al., 1989) algorithms. The unfolding and refolding data as a function of peptide and/or Gdn-HCl concentration were fit to the kinetic scheme:

$$N_2 \underset{k_f}{\overset{k_u}{\rightleftharpoons}} 2U \quad (3)$$

where U is the unfolded monomer, N_2 is the native dimer, and k_f and k_u are the rate constants for the folding and unfolding reactions, respectively. Concentrations of the two species as a function of time were obtained by numerical integration of the rate equations using a second-order Runge−Kutta algorithm with an adaptive step size control (Press et al., 1989). A numerical integration algorithm was chosen to facilitate implementation of more complex models, including those involving a monomeric or dimeric intermediate. For the analysis of the Gdn-HCl dependence of the folding rates, it was assumed that the activation free energies depended linearly on denaturant concentration (Matthews, 1987). Thus, the corresponding dependence of the rate constants on denaturant concentration is described by

$$k = k_{H_2O} e^{-m[D]/RT} \quad (4)$$

where k_{H_2O} is the rate constant for folding or unfolding in the absence of denaturant, m is the parameter describing the Gdn-HCl dependence of the activation free energy, [D] is the denaturant concentration, R is the gas constant, and T is the temperature.

When all of the kinetic traces were fit simultaneously, the following parameters were globally constrained: the rate constants for folding, k_{f,H_2O}, and unfolding, k_{u,H_2O}, in the absence of denaturant, and the parameters representing the Gdn-HCl dependence of the rate constants for folding, m_f, and unfolding, m_u. The molar ellipticities of the unfolded monomer, $[\theta_U]$, and native dimer, $[\theta_D]$, the temperature, T, the denaturant concentration, D, and the initial fraction of unfolded monomer (equal to 1 for refolding data and 0 for unfolding data) were fixed parameters. In initial fitting efforts, the peptide concentrations were fixed; however, small inconsistencies (<10%) were observed between the expected peptide concentrations and the asymptotic value of the kinetic trace. Because the association rate constant is peptide concentration dependent, it was necessary to define the total peptide concentration as an adjustable local parameter. This approach allowed for slight variations in peptide concentration resulting either from errors in estimating the initial concentration from the extinction coefficient or errors from inaccurate syringe dilutions. The resulting peptide concentrations used in the fits were within the estimated uncertainty (10%) of the expected concentrations.

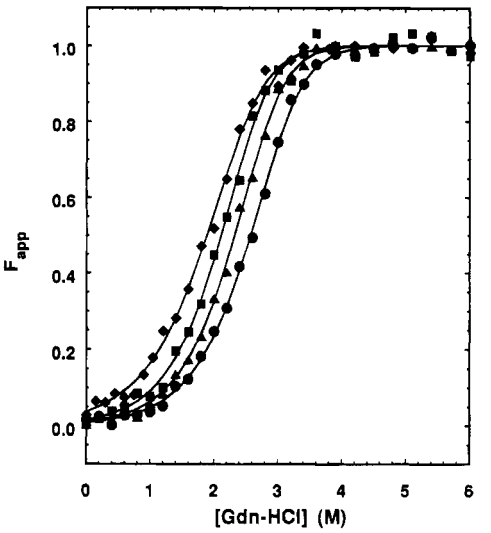

FIGURE 1: Dependence of the apparent fraction of unfolded protein, $F_{app} = (\theta_O - \theta_N)/(\theta_U - \theta_N)$, on the Gdn-HCl concentration at pH 7.0 and 5 °C. The monomer peptide concentrations are 6 (♦), 12.4 (■), 17.6 (▲), and 37.5 μM (●), respectively. Lines represent fits of the data to a two-state model using eq 2.

The data were also globally fit to kinetic models containing a monomeric or dimeric intermediate. In choosing the most appropriate model, three criteria were considered: (1) the statistical quality of the fit as reflected in the reduced chi-squared (χ_r^2) values (Bevington, 1969), (2) the randomness of the residual plots, and (3) the feasibility of the resulting parameters. In some cases, an offset constant was included in the model function to compensate for instrumental drift between data sets. All kinetic models were tested with and without using an offset parameter. This constant, which was typically within ±2 mdeg, served to improve the quality of the fits and led to more accurate values for the peptide concentrations but did not have any significant effect on the rate constants or slopes obtained in any of the models tested.

RESULTS

Equilibrium Unfolding Studies. The circular dichroism spectrum of GCN4-p1 at 5 °C exhibits the characteristic α-helical spectrum with a double minimum at 222 and 208 nm (Woody, 1985). The mean residue ellipticity of this peptide at 222 nm is $-3.3 \pm 0.3 \times 10^4$ deg cm^2 dmol^{-1}, very similar to that reported previously for GCN4-p1 (O'Shea et al., 1989) and consistent with an essentially 100% helical structure in the dimeric peptide (Woody, 1985). The equilibrium unfolding of the peptide was followed by monitoring the dependence of the ellipticity at 222 nm on the concentration of Gdn-HCl at 5 °C. As the Gdn-HCl concentration is increased, the CD signal decreases in a sigmoidal fashion, indicative of a cooperative unfolding transition (Figure 1). The equilibrium unfolding transition

Table 1: Free Energy of Unfolding of GCN4-p1 as a Function of Peptide Concentration at pH 7.0 and 5 °C

	[GCN4-p1][a] (μM)	$\Delta G°$ H_2O[b] [kcal (mol dimer)$^{-1}$]	$-m$[c] [kcal mol^{-1} (molar Gdn)$^{-1}$]	C_m[d] (M)
	6.0	9.88 ± 0.71	1.71 ± 0.26	1.89
	12.4	10.46 ± 0.71	1.99 ± 0.26	2.12
	12.6	10.54 ± 0.60	1.96 ± 0.22	2.19
	17.6	10.68 ± 0.43	1.99 ± 0.15	2.33
	37.5	10.50 ± 0.37	1.88 ± 0.12	2.58
local (ave.)		10.49 ± 0.23	1.91 ± 0.08	
global		10.24 ± 0.38	1.82 ± 0.12	
kinetics		10.31 ± 0.19	1.84 ± 0.05	

[a] Peptide concentrations are expressed in terms of total concentration of monomer. [b] $\Delta G°_{H_2O}$ is the free energy of unfolding of the dimer in the absence of denaturant. [c] m denotes the Gdn-HCl dependence on the free energy of folding, $\Delta G° = \Delta G°_{H_2O} + m[D]$, and reflects the cooperativity of the folding reaction. [d] The midpoint of the unfolding transition ($F_{app} = 0.5$) is calculated from eq 2. Errors in C_m are estimated to be ±0.05. Errors in the peptide concentrations are ±10%. All other errors are 95% confidence levels.

is fully reversible as demonstrated by the complete recovery of the ellipticity at 222 nm upon dilution of the denaturant (data not shown). The relationship of this conformational transition to a dimer/monomer equilibrium was tested by repeating the Gdn-HCl titration at a series of GCN4-p1 concentrations which span the final concentrations used in the kinetic experiments (Figure 1). The progressive increase in the midpoint of the transition as the peptide concentration is increased is consistent with that predicted from a dimer/monomer equilibrium.

The validity of a two-state model can be quantitatively assessed by fitting these data to eq 2 as described in Materials and Methods. In these fits, it was assumed that the ellipticities of the native and unfolded forms and the free energy of unfolding depend linearly on the denaturant concentration (Shellman, 1978; Pace, 1986). The excellent agreement between observed and predicted denaturation curves at four different peptide concentrations (Figure 1) and the consistent value of the free energy of unfolding obtained over this 6-fold peptide concentration range (Table 1) demonstrate that a two-state model provides an accurate description of this system. The free energy of unfolding of the dimer under standard state conditions is 10.49 ± 0.23 kcal (mol dimer)$^{-1}$ and the cooperativity parameter is −1.91 ± 0.08 kcal mol^{-1} (molar Gdn-HCl)$^{-1}$ at 5 °C and pH 7.0. A global fit of all five data sets yields values of 10.24 ± 0.38 kcal (mol dimer)$^{-1}$ and −1.82 ± 0.12 kcal mol^{-1} (molar Gdn-HCl)$^{-1}$, respectively. The free energy of unfolding for GCN4-p1 is comparable to that observed for many other much larger dimeric proteins (Neet & Timm, 1994) and represents remarkable stability for such a small peptide (Pace, 1990).

Kinetic Folding Studies. Having demonstrated that Gdn-HCl induces a native dimer/unfolded monomer transition in GCN4-p1, kinetic refolding jumps were performed at a series of final peptide concentrations to examine the association reaction. Throughout the peptide concentration range studied, the mean residue ellipticities of the unfolded peptides were ~0−500 deg cm^2 dmol^{-1} in 5 M Gdn-HCl. Thus, the peptide is essentially completely unfolded at the start of a kinetic jump from this solvent. Under the final refolding conditions (0.5 M Gdn-HCl), the peptides are >92% folded as judged by the equilibrium unfolding curves (Figure 1).

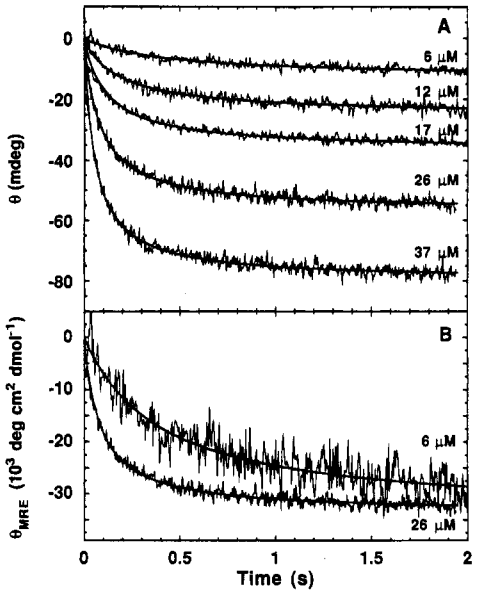

FIGURE 2: (A) Kinetic traces observed under strongly refolding conditions by stopped-flow CD. The ellipticity at 222 nm is shown as a function of refolding time for five different monomer concentrations. The final concentration of Gdn-HCl was 0.5 M after a rapid 10-fold dilution of unfolded peptide in 5 M Gdn-HCl. Lines represent local fits to the model, $2U \xrightarrow{k_f} N_2$, neglecting the back-reaction. (B) Normalized kinetic traces at two different monomer peptide concentrations, 6 and 26 μM, plotted as mean residue ellipticity as a function of time.

The mean residue ellipticities observed at the endpoints of the kinetic traces match very well with those observed at equilibrium (~−33 000 deg cm^2 dmol^{-1}, data not shown), indicating that folding is also reversible under the conditions of the kinetic experiments.

A subset of the refolding traces obtained by monitoring the ellipticity at 222 nm is shown in Figure 2A. The kinetics exhibit a noticeable dependence on peptide concentration, as demonstrated by an increasing rate of the refolding reaction with increasing peptide concentration. This behavior is more clearly displayed in Figure 2B, where the time dependence at two extreme peptide concentrations is plotted on a normalized scale to account for increases in ellipticity with increasing peptide concentration. Under strongly refolding conditions (0.5 M final Gdn-HCl concentration), local fits of each individual kinetic trace to the simple bimolecular association reaction, $2U \xrightarrow{k_f} N_2$, yield a second-order rate constant of 2.16 ± 0.38 × 10^5 M^{-1} s^{-1}. No systematic dependence of the rate constant on peptide concentration was observed, indicating that the data is well described by a simple bimolecular association reaction throughout the entire concentration range examined. Extrapolations of these kinetic traces to zero time according to these second-order rate constants gave predicted ellipticities which closely match those expected for the unfolded, monomeric peptide. Local fits of the data over the entire peptide concentration range investigated demonstrate that less than 10% of the far-UV CD signal develops in the first 5 ms of folding. A global fit of all of the peptide concentration data (22 kinetic traces with monomer concentrations ranging from 6 to 38 μM) yields a rate constant of 1.94 ± 0.21 × 10^5 M^{-1} s^{-1} in 0.5 M Gdn-HCl.

The guanidine hydrochloride dependence of both the refolding and unfolding reactions were determined in an

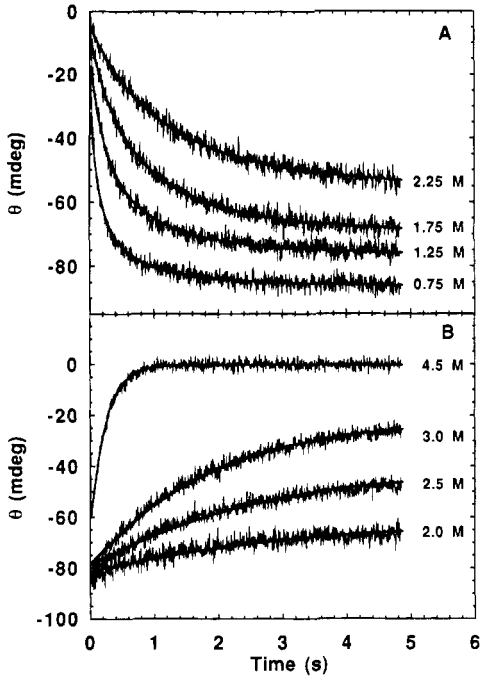

FIGURE 3: Kinetic refolding (A) and unfolding (B) traces at various final Gdn-HCl concentrations and constant peptide concentration (38 μM), monitored by the change in ellipticity at 222 nm with time at pH 7.0 and 5 °C. Solid lines represent global fits to the model, $N_2 \underset{k_f}{\overset{k_u}{\rightleftharpoons}} 2U$.

effort to highlight possible intermediates in the folding mechanism. Refolding was initiated by a rapid 10-fold dilution of GCN4-p1 into various final concentrations of Gdn-HCl. Likewise, the unfolding reaction was examined by a rapid 5-fold dilution of the peptide in buffer with concentrated Gdn-HCl solutions. Usable unfolding data, however, were only obtained when utilizing two of the three Biologic syringes. This procedure requires the solution to flow through two mixers, presumably improving the homogeneous mixing of highly viscous Gdn-HCl solutions. Although this procedure increased the dead-time of mixing from 5 to 14 ms, it did not interfere with the collection of data because the unfolding of GCN4-p1 occurred on a substantially slower time scale.

Representative subsets of the refolding and unfolding kinetic traces at various final Gdn-HCl concentrations are shown in Figure 3. Inspection of the kinetic traces indicated that the refolding rate steadily decreased as the final Gdn-HCl concentration was increased from 0.75 to 2.25 M (Figure 3A). Correspondingly, the unfolding rate progressively increased as the final Gdn-HCl concentration was increased from 2.0 to 4.5 M (Figure 3B).

Local fits of the refolding kinetic traces to the simple model $2U \xrightarrow{k_f} N_2$ were performed from 0.5 to 1.5 M Gdn-HCl, a final denaturant concentration range where the unfolding rate was not expected to contribute significantly. The Gdn-HCl dependence of the apparent association rate constant between 0.5 and 1.5 M Gdn-HCl is shown in Figure 4 (closed symbols) for two different monomer peptide concentrations, 12 and 38 μM. The linear dependence of the rate constant on Gdn-HCl concentration demonstrates that refolding is well described by a simple bimolecular association reaction in this region.

Under strongly unfolding conditions (final concentrations

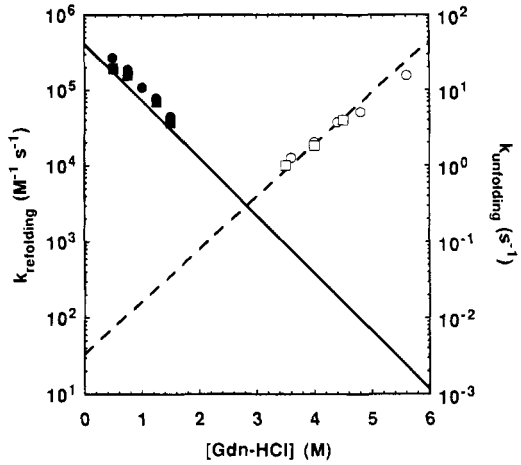

FIGURE 4: Gdn-HCl dependence of the rate constants for refolding (solid line) and unfolding (dashed line). Lines represent the results of a global fit of 90 kinetic traces, both unfolding and refolding as a function of both Gdn-HCl concentration and peptide concentration, to the model $N_2 \underset{k_f}{\overset{k_u}{\rightleftharpoons}} 2U$ ($\chi_r^2 = 1.28$). Symbols represent local fits to the refolding model, $2U \xrightarrow{k_f} N_2$ (closed symbols) or unfolding model, $N_2 \xrightarrow{k_u} 2U$ (open symbols) at 12 (circles), or 38 μM (squares) peptide concentration. The errors in the local fits are represented by the size of the symbols.

of Gdn-HCl ≥3.5 M), the kinetics are well described by a single phase whose rate constant increases exponentially with increasing Gdn-HCl concentration (Figure 4, open symbols). The amplitude of this kinetic phase agrees well with the value expected from the equilibrium unfolding process (data not shown). The close agreement demonstrates that there are no fast unfolding phases which occur within the dead-time of mixing. Deviations from a simple exponential dependence occur in the transition region (data not shown) because the refolding reaction begins to contribute significantly to the observed relaxation time. The unfolding kinetics were shown to be independent of peptide concentration by measuring the relaxation time at two different monomer peptide concentrations, 12 and 38 μM. Above 3 M Gdn-HCl, the measured relaxation times were within experimental error for both peptide concentrations (Figure 4).

To determine whether these simple unfolding and refolding kinetic schemes could be combined to provide an accurate description of the folding of GCN4-p1 under all of the conditions studied, a global kinetic analysis of all of the refolding and unfolding data was performed by simultaneously fitting 90 kinetic traces, with 1000 data points each, to the simple model, $N_2 \underset{k_f}{\overset{k_u}{\rightleftharpoons}} 2U$. A global analysis of the data has the advantage of overdetermination of model parameters, which aids in discerning between competing models and accurately determining the microscopic rate constants (Knutson et al., 1983). The data sets used in this analysis were selected to reflect a range of folding conditions: peptide concentration data under strongly refolding conditions and Gdn-HCl-dependent refolding and unfolding kinetic traces at 12 and 38 μM monomer peptide concentration. The guanidine dependence of the kinetic data was incorporated into the global analysis by assuming that the activation free energies of unfolding and refolding depend linearly on denaturant concentration (Matthews, 1987). This assumption is supported by the observed exponential dependence of the unfolding and refolding relaxation times on the

denaturant concentration obtained from local fits in the appropriate baseline regions (Figure 4, symbols). The Gdn-HCl dependence of the molar ellipticities for native dimer and unfolded monomer were not included as additional parameters because the slopes of the native and unfolded baselines obtained from equilibrium unfolding titrations are essentially zero (data not shown).

Comparison of predicted and observed kinetic traces throughout the entire Gdn-HCl range for both refolding and unfolding shows, in general, excellent agreement (Figure 3, solid lines). To test whether or not small deviations at early times in some cases could result from the presence of an intermediate, the data were also fit to kinetic models containing either a dimeric or a monomeric intermediate along the refolding pathway. These kinetic models gave statistically insignificant improvements in the fits (χ_r^2 = 1.27), and the additional parameters were rendered redundant. In the case of a monomeric intermediate, the molar ellipticity obtained was nearly equivalent to the molar ellipticity of the unfolded form, and the rate of formation of the monomer was predicted to occur within the dead-time of the experiment. The extinction coefficient obtained for a dimeric intermediate was 98% that of the native dimer, effectively collapsing the three-state model to a two-state model. It can be concluded that the simple two-state kinetic model provides an accurate description of the Gdn-HCl-induced unfolding and refolding of GCN4-p1.

The dependence of the unfolding and refolding rate constants on denaturant concentration, obtained from the global analysis, is depicted in Figure 4 (dashed and solid line, respectively). The good agreement between the rate constants obtained by local and global fits of the data supports the validity of the global analysis. Although the consistently larger values for the refolding rate constants obtained from the local fits are within experimental error of those from the global analysis, this difference may also reflect the presence of a small amount of an intermediate species. However, as noted above, there is no strong statistical support for either a monomeric or dimeric intermediate. The bimolecular association rate in the absence of denaturant, k_{f,H_2O}, is 4.18 ± 0.78 × 10^5 M^{-1} s^{-1}, and the corresponding unfolding rate constant, k_{u,H_2O}, is 3.34 ± 0.54 × 10^{-3} s^{-1}. The guanidine dependence of the activation free energies of refolding and unfolding yield m values of 0.966 and −0.877, respectively.

As a further test of the validity of the simple two-state kinetic model, the rate constants and slopes obtained from the global fit were used to independently predict the equilibrium unfolding curve. The equilibrium curves for 13 and 38 μM peptide predicted from the kinetics are compared with the actual equilibrium titrations at the same peptide concentrations in Figure 5. The excellent agreement at both concentrations strongly supports the two-state kinetic model. The free energy of unfolding calculated from the ratio of the kinetic rate constants, i.e., the equilibrium constant, is 10.31 ± 0.19 kcal (mol dimer)$^{-1}$, in excellent agreement with the free energy of unfolding determined independently from equilibrium Gdn-HCl titration experiments (Table 1). Similarly, the cooperativity parameter of the unfolding transition, m, calculated from the slopes of the guanidine dependence of the rate constants for refolding and unfolding [$m = m_u - m_f = -1.84$ kcal mol^{-1} (molar Gdn-HCl)$^{-1}$] is very close to that of the equilibrium measurement, −1.91 kcal mol^{-1} (molar Gdn-HCl)$^{-1}$. On the basis of secondary structure, the Gdn-HCl-induced folding of GCN4-p1 only involves significant populations of the native dimer and unfolded monomer.

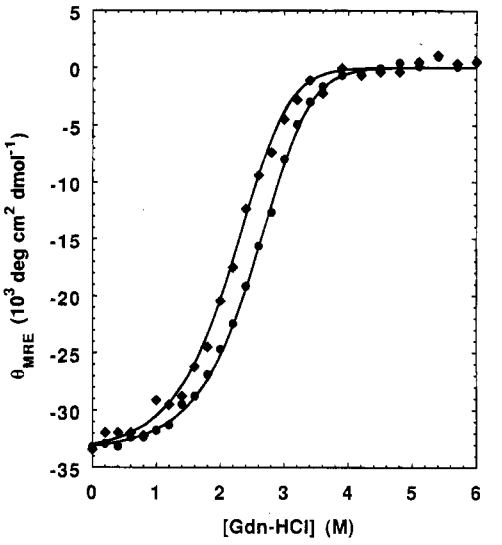

FIGURE 5: Simulation of the equilibrium unfolding curve from the kinetic data at two different monomer concentrations. The solid line results from a combined fit of all of the unfolding and refolding data, and the symbols represent equilibrium data points taken at 13 (♦) and 38 μM (●) peptide, respectively.

DISCUSSION

The guanidine-induced unfolding and refolding of the leucine zipper peptide GCN4-p1, as monitored by stopped-flow circular dichroism spectroscopy, are well described by two-state equilibrium and kinetic models. This result is consistent with the thermal melting of a somewhat larger peptide containing the same dimerization domain, which was also found to follow a two-state equilibrium model (Thompson et al., 1993). The absence of stable and/or transient folding intermediates, which could provide clues to the mechanism, differentiates this simple dimeric system from many larger proteins (Kim & Baldwin, 1990; Matthews, 1993). This behavior is, however, similar to that of several small, monomeric proteins, including chymotrypsin inhibitor-2 (Jackson & Fersht, 1991), cytochrome *c* (Sosnick et al., 1994), and the IgG-binding domain of streptococcal protein G (Alexander et al., 1992), and to that of the small dimeric *arc* repressor under strongly folding conditions at low protein concentrations (<16 μM) (Milla & Sauer, 1994). The observation of two-state folding kinetics, however, does not mean that these proteins fold by a random search. Rather, this simple response only demonstrates that partially folded forms are not sufficiently stable relative to the unfolded form to become measurably populated during folding under these conditions.

For the folding of GCN4-p1 in particular and coiled coils in general, it is reasonable to suppose that some preorganization of a monomer species may be required to lead to productive dimerization. For example, the development of an extensive hydrophobic interface may require that the peptide adopt a helical conformation. Computer simulations on the folding of GCN4-p1 suggest that dimer formation follows the collision of short helical stretches of residues in the monomer chains with an initial helix content of about

30% (Vieth et al., 1994). These helical stretches are then predicted to propagate along the molecule until the final coiled-coil dimer with a helix content of ~90% is formed. The inability to detect a folded monomeric species by CD in the present study, however, shows that any unfolded/folded monomer equilibrium must strongly favor the unfolded form.

While the current study also reveals no kinetic evidence for a unimolecular rearrangement step following dimerization, such a conformational reorganization has been observed previously in the folding of an analogue of GCN4-p1 probed by fluorescence (Wendt et al., 1994). When the monomer/dimer equilibrium of a fluorescently labeled derivative of GCN4-p1 was perturbed by dilution of the fully native conformation in the absence of denaturant, Bosshard and his colleagues observed two first-order phases but no second-order phase. There are several possible explanations for the potential discrepancy resulting from the absence of a kinetically detectable dimeric intermediate in the present study. First, circular dichroism, which is a global probe of secondary structure, may be insensitive to local conformational effects detected by fluorescence. Second, the fluorescein probe used in the fluorescence studies may itself favor alternatively folded structures. Third, in the current study, the presence of 0.5 M Gdn-HCl in the final refolded solution may be sufficient to destabilize any potential dimeric intermediates. A similar situation has been observed in the thermal unfolding of dihydrofolate reductase, which exhibits a three-state equilibrium in aqueous buffer but only a two-state equilibrium in the presence of low concentrations of denaturant (J.L. and C.R.M., unpublished results).

The predicted second-order refolding rate constant for GCN4-p1 in the absence of denaturant, 4.2×10^5 M^{-1} s^{-1}, is 3−4 orders of magnitude smaller than one might expect for the random collision of two peptides of this size in solution (Amdur & Hammes, 1966). Although it is usually observed that bimolecular rate constants in biology are substantially less than those expected for the collision of two spheres (Berg & von Hippel, 1985), the association/folding rate constant for the larger (53 residues per monomer), structurally more complex *arc* repressor is 20-fold larger than that of GCN4-p1 (Milla & Sauer, 1994). Moreover, the bimolecular rate constant for the highly intertwined, dimeric *trp* aporepressor (108 residues per monomer), which is known to fold through a stable monomeric form (Mann & Matthews, 1993), approaches the diffusion limit of $\sim 10^9$ M^{-1} s^{-1} (X. Shao and C.R.M., unpublished results).

The wide variation in second-order rate constants in these and other systems (Koren & Hammes, 1976) may reflect the way in which folding and association are coupled in these dimeric systems. If folding (or at least partial folding) of a monomer is required for association and if this folding/unfolding reaction is very fast, the subsequent association reaction will have an apparent second-order rate constant whose magnitude reflects the position of the monomer folding reaction. The larger the fraction of folded monomer, i.e., the association-competent form, the greater the observed bimolecular rate constant. The relatively small bimolecular rate constant observed for GCN4-p1 suggests that association might involve an unstable, poorly populated monomeric intermediate, a proposal that is consistent with the absence of a burst phase signal in the stopped-flow CD experiment (Figures 2 and 3). The second-order rate observed for GCN4-p1 is comparable to the bimolecular association rate constants observed for complementary fragments of the monomeric proteins chymotrypsin (de Prat Gay et al., 1994) and barnase (Kippen et al., 1994), where one or both of the isolated fragments in these two proteins do not fold significantly. By contrast, the fast association rate constant ($>8 \times 10^7$ M^{-1} s^{-1}) estimated for tropomyosin (Mo et al., 1991a) may reflect a higher probability of forming a helical stretch in the longer monomer chain (Poland & Scheraga, 1970).

The simplicity of the folding mechanism of GCN4-p1 suggests that it should serve as an excellent model for exploring the contributions of various noncovalent interactions to the folding and association of this dimeric peptide. Amino acid replacements at the dimer interface would be expected to primarily perturb the association reaction while those on the surface would perturb the putative helix/coil transition in the monomeric peptide. Such experiments would provide a means of directly testing the hypothesis that the apparent associate rate constant for protein−protein interactions is influenced by the extent of folding of the monomer chains. The results obtained on GCN4-p1 might provide useful insights into the development of quaternary structure in much more complex multisubunit proteins.

ACKNOWLEDGMENT

We are grateful to Dr. S. Marqusee for the gift of the GCN4-p1 peptide and T. M. Raschke for deprotecting the peptide and cleaving it from the resin. We are indebted to Dr. D. Lambright for sharing Savuka, the analysis package to which our fitting routines were interfaced. Electrospray mass spectrometry was performed by D. King at the peptide facility at the University of California, Berkeley. Peptide for preliminary studies which motivated this work was provided by Dr. P. S. Kim. We thank Dr. T. Alber for continuing and insightful contributions and Dr. C. V. Gegg for helpful discussions and a critical review of the manuscript.

REFERENCES

Alexander, P., Orban, J., & Bryan, P. (1992) *Biochemistry 31*, 7243−7248.
Amdur, I., & Hammes, G. G. (1966) *Chemical Kinetics: Principles and Selected Topics*, McGraw-Hill, New York.
Berg, O. G., & von Hippel, P. H. (1985) *Annu. Rev. Biophys. Biophys. Chem. 14*, 131−160.
Bevington, P. R. (1969) *Data Reduction and Error Analysis for the Physical Sciences*, McGraw Hill, New York.
Blond, S., & Goldberg, M. E. (1985) *J. Mol. Biol. 182*, 597−606.
Crick, F. H. C. (1953) *Acta Crystallogr. 6*, 689−697.
Cohen, C., & Parry, D. A. D. (1986) *Trends Biochem. Sci. 11*, 245−248.
Cohen, C., & Parry, D. A. D. (1990) *Proteins 7*, 1−15.
DeGrado, W. F. (1988) *Adv. Protein Chem. 39*, 51−124.
Edelhoch, H. (1967) *Biochemistry 6*, 1948−1954.
Ellenberger, T. (1994) *Curr. Opin. Struct. Biol. 4*, 12−21.
Garel, J. R. (1992) in *Protein Folding* (Creighton, T. E., Ed.) pp 405−454, Freeman, New York.
Gittelman, M. S., & Matthews, C. R. (1990) *Biochemistry 29*, 7011−7020.
Goodman, E. M., & Kim, P. S. (1991) *Biochemistry 30*, 11615−11620.
Harbury, P. B., Zhang, T., Kim, P. S., & Alber, T. (1993) *Science 262*, 1401−1407.
Harbury, P. B., Kim, P. S., & Alber, T. (1994) *Nature 371*, 80−83.
Holtzer, M. E., Holtzer, A., & Skolnick, J. (1983) *Macromolecules 16*, 173−180.
Jackson, S. E., & Fersht, A. R. (1991) *Biochemistry 30*, 10436−10443.

Jaenicke, R. (1987) *Prog. Biophys. Mol. Biol. 49*, 117−237.
Jaenicke, R. (1991) *Biochemistry 30*, 3147−3161.
Kim, P. S., & Baldwin, R. L. (1990) *Annu. Rev. Biochem. 59*, 631−660.
Kippen, A. D., Sancho, J., & Fersht, A. R. (1994) *Biochemistry 33*, 3778−3786.
Knutson, J. R., Beechem, J. M., & Brand, L. (1983) *Chem. Phys. Lett. 102*, 501−507.
Koren, R., & Hammes, G. G. (1976) *Biochemistry 15*, 1165−1171.
Lehrer, S. S. (1978) *J. Mol. Biol. 118*, 209−226.
Mann, C. J., & Matthews, C. R. (1993) *Biochemistry 32*, 5282−5290.
Marquardt, D. W. (1963) *J. Soc. Ind. Appl. Math. 11*, 431−441.
Matthews, C. R. (1987) *Methods Enzymol. 154*, 498−511.
Matthews, C. R. (1993) *Annu. Rev. Biochem. 62*, 653−683.
Milla, M. E., & Sauer, R. T. (1994) *Biochemistry 33*, 1125−1133.
Mo, J., Holtzer, M. E., & Holtzer, A. (1991a) *Proc. Natl. Acad. Sci. U.S.A. 88*, 916−920.
Mo, J., Holtzer, M. E., & Holtzer, A (1991b) *Biopolymers 31*, 1417−1427.
Monera, O. D., Zhou, N. E., Kay, C. M., & Hodges, R. S. (1993) *J. Biol. Chem. 268*, 19218−19227.
Munson, M., O'Brien, R., Sturtevant, J., & Regan, L. (1994) *Protein Sci. 3*, 2015−2022.
Myszka, D. G., & Chaiken, I. M. (1994) *Biochemistry 33*, 2363−2372.
Neet, K. E., & Timm, D. E. (1994) *Protein Sci. 3*, 2167−2174.
Oas, T. G., McIntosh, L. P., O'Shea, E. K., Dahlquist, F. W., & Kim, P. S. (1990) *Biochemistry 29*, 2891−2894.
O'Shea, E. K., Rutkowski, R., & Kim, P. S. (1989) *Science 243*, 538−542.
O'Shea, E. K., Klemm, J. D., Kim, P. S., & Alber, T. (1991) *Science 254*, 539−544.
Pace, C. N. (1986) *Methods Enzymol. 131*, 266−280.
Pace, C. N. (1990) *Trends Biochem. Sci. 15*, 14−17.
Poland, D., & Scheraga, H. A. (1970) *Theory of Helix−Coil Transitions in Biopolymers, Statistical Mechanical Theory of Order−Disorder Transitions in Biological Macromolecules*, Academic Press, New York.
Prat Gay, G. de, Ruiz-Sanz, J., & Fersht, A. R. (1994) *Biochemistry 33*, 7964−7970.
Press, W. H., Flannery, B. P., Teukolsky, S. A., & Vetterling, W. T. (1989) *Numerical Recipes: The Art of Scientific Computing (FORTRAN Version)* Cambridge University Press, Cambridge, U.K.
Regan, L., & DeGrado, W. F. (1988) *Science 241*, 976−978.
Rozzelle, J. E., Jr., Tropsha, A., Erickson, B. W. (1994) *Protein Sci. 3*, 345−355.
Schellman, J. A. (1978) *Biopolymers 17*, 1305−1322.
Schildbach, J. F., Milla, M. E., Jeffrey, P. D., Raumann, B. E., & Sauer, R. T. (1995) *Biochemistry 34*, 1405−1412.
Sosnick, T. E., Mayne, L., Hiller, R., & Englander, S. W. (1994) *Struct. Biol. 1*, 149−156.
Thompson, K. S., Vinson, C. R., & Freire, E. (1993) *Biochemistry 32*, 5491−5496.
Tonomura, B., Nakatani, H., Ohnishi, M., Yamaguchi-Ito, J., & Hiromi, K. (1978) *Anal. Biochem. 84*, 370−383.
Vieth, M., Kolinski, A., Brooks, C. L., III, & Skolnick, J. (1994) *J. Mol. Biol. 237*, 361−367.
Wendt, H., Baici, A., & Bosshard, H. R. (1994) *J. Am. Chem. Soc. 116*, 6973−6974.
Wendt, H., Berger, C., Baici, A., Thomas, R. M., & Bosshard, H. R. (1995) *Biochemistry 34*, 4097−4107.
Woody, R. W. (1985) *The Peptides 7*, 15−114.
Zetina, C. R., & Goldberg, M. E. (1982) *J. Mol. Biol. 157*, 133−148.
Ziegler, M. M., Goldberg, M. E., Chaffotte, A. F., & Baldwin, T. O. (1993) *J. Biol. Chem. 268*, 10760−10765.
Zhou, N. E., Kay, C. M., & Hodges, R. S. (1994) *J. Mol. Biol. 237*, 500−512.

BI951469N